Available online at www.sciencedirect.com
SCIENCE DIRECT®
PERGAMON
Polyhedron 22 (2003) 2799–2807
POLYHEDRON
www.elsevier.com/locate/poly

Bimetallic transition metal–ruthenium(II) complexes containing bridging bipyrimidine ligands

Carla D. Nunes [a], Martyn Pillinger [a], Alan Hazell [b], Josua Jepsen [b], Teresa M. Santos [a,*], João Madureira [a], André D. Lopes [c], Isabel S. Gonçalves [a,*]

[a] Department of Chemistry, CICECO, University of Aveiro, 3810-193 Aveiro, Portugal
[b] Department of Chemistry, University of Aarhus, Langelandsgade 140, DK-8000 Aarhus C, Denmark
[c] Department of Chemistry, Faculty of Science and Technology, University of the Algarve, Campus de Gambelas, 8000-117 Faro, Portugal

Received 28 April 2003; accepted 13 June 2003

Abstract

The ruthenium(II) complex $[Ru([14]aneS_4)(bpym)](BF_4)_2$ ([14]aneS$_4$ = 1,4,8,11-tetrathiacyclotetradecane, bpym = 2,2′-bipyrimidine) has been prepared by substitution of the labile acetonitrile ligands in the complex $[Ru([14]aneS_4)(CH_3CN)_2](BF_4)_2$ by bpym. Both the precursor acetonitrile complex and the polypyridyl complex were characterised by Ru *K*-edge EXAFS spectroscopy. In addition, the crystal structures of $[Ru([14]aneS_4)(bpym)](X)_2$ (X = BF_4, PF_6) were determined by X-ray diffraction. The bpym-bridged bimetallic complexes $[\{Ru([14]aneS_4)\}_2(bpym)](BF_4)_4$ and $[\{([14]aneS_4)Ru\}(bpym)\{ReO_3Me\}](BF_4)_2$ were prepared using the ruthenium(II) monomeric bpym complex as starting material. In the case of the complex containing methyltrioxorhenium(VII) coordination of both metal centres to the bidentate bridging ligand was supported by a combination of Ru *K*-edge and Re *L*-edge XAFS spectroscopy, in addition to ^{1}H NMR.

Keywords: Ruthenium; N ligand; Bridging ligands; Heterometallic complexes; EXAFS spectroscopy

1. Introduction

Heterobimetallic or polymetallic complexes in which the metal centres interact through ligand bridges have potential applications in such diverse areas as catalysis, materials, medicine and sensor technology [1]. Variation of the metal centres or ligands can lead to a tailoring of the spectroscopic and redox properties. Compounds bridged by polypyridyl ligands are particularly attractive as these ligands can facilitate metal–metal communication. Common examples are 2,3-bis(2-pyridyl)pyrazine (dpp) [2,3], bisimidazole (H_2Biim) [4], and 2,2′-bipyrimidine (bpym) [3,5–7]. The bpym ligand is able to bridge a variety of metal centres and is expected to electronically couple adjacent metal centres in a polymetallic system [5]. This coupling is due to the ligands ability to position two metal centres at a distance of approximately 5.5 Å in a fixed orientation which will allow an indirect dπ–dπ interaction.

Recently, some of us reported on binuclear molybdenum(II)–rhenium(VII) complexes with nitrogen donor bridges [8]. The complexes $[\{CpMo(CO)_2\}(\mu\text{-Biim})\{Re(X)O_3\}]Na$ and $[\{Cp_2Mo\}(\mu\text{-Biim})\{Re(X)O_3\}]$ (X = Cl, CH_3) were prepared by reaction of, respectively, the anion $[CpMo(CO)_2(Biim)]^-$ and the neutral compound $Cp_2Mo(Biim)$ with $XReO_3$. These complexes are particularly interesting due to the combination of metals in high and low oxidation states. In related work, the binuclear molybdenum(II)–molybdenum(VI) compound $[CpMo(CO)_2(bpym)MoO_2Br_2]BF_4$ was prepared from $[CpMo(CO)_2(bpym)]BF_4$ and $MoO_2Br_2(CH_3CN)_2$ [9]. In this example, the donor capability of the bpym ligand is enhanced by combining it with the organometallic fragment.

In the present work, the acetonitrile complex $[Ru([14]aneS_4)(CH_3CN)_2](BF_4)_2$ ([14]aneS$_4$ = 1,4,8,11-tetrathiacyclotetradecane) has been used as a starting material for the preparation of the complex [Ru([14]-

* Corresponding authors. Tel.: +351-234-37-0200; fax: +351-234-37-0084 (I.S.G.).
E-mail address: igoncalves@dq.ua.pt (I.S. Gonçalves).

0277-5387/03/$ - see front matter © 2003 Elsevier Science Ltd. All rights reserved.
doi:10.1016/S0277-5387(03)00397-8

aneS$_4$)(bpym)](BF$_4$)$_2$, the structure of which has been determined by single crystal X-ray diffraction. We have explored the utility of this complex as a precursor for the formation of bimetallic systems. As a result, the binuclear complexes [{Ru([14]aneS$_4$)}$_2$(bpym)](BF$_4$)$_4$ and [{([14]aneS$_4$)Ru}(bpym){ReO$_3$Me}](BF$_4$)$_2$ have been isolated and characterised. In these two examples, the cationic fragment [Ru([14]aneS$_4$)(bpym)]$^{2+}$ is acting as a 'metalloligand', that is, binding a second metal at the free coordination site. In the case of the trioxorhenium(VII) fragment, X-ray absorption fine structure spectroscopy has been used to confirm the formation of a true ligand bridged heterobimetallic complex.

2. Results and discussion

2.1. Preparation and spectroscopic characterisation of monomeric ruthenium(II) complexes

The pale yellow complex [Ru([14]aneS$_4$)(CH$_3$CN)$_2$](BF$_4$)$_2$ (**1**) was prepared as described previously by refluxing a solution of [Ru([14]aneS$_4$)(DMSO)Cl]Cl in acetonitrile in the presence of TlBF$_4$ [10]. Treatment of **1** with 1 equiv. of bpym in ethanol gives an orange solution from which the product [Ru([14]aneS$_4$)(bpym)](BF$_4$)$_2$ (**2a**) was isolated as an analytically pure orange crystalline solid in good yield (Scheme 1). The IR spectrum of **2a** in the solid state does not contain an absorption band (at 2284 cm^{-1}) for the C≡N stretch of coordinated acetonitrile molecules. Instead, the presence of coordinated bpym is indicated by bands at 1574 and 1555 cm^{-1} (1577 and 1552 cm^{-1} in the Raman spectrum) due to C=C and C=N pyrimidine ring stretching vibrations. Non-coordinated ('free') bpym presents only one IR band in this region at 1556 cm^{-1} (1562 cm^{-1} in the Raman spectrum). The electronic spectrum of complex **2** dissolved in acetonitrile features a UV–Vis pattern similar to that seen for analogous Ru^{II} thioether polypyridyl complexes, such as [Ru([12]aneS$_4$)(2,2′-bipyridyl)]Cl$_2$ [11]. Intense high energy bipyrimidine-based π→π* bands occur at 201 and 264 nm. A metal-to-ligand charge transfer Ru^{II} (dt_{2g})→π* transition appears at 415 nm and the band at 332 nm can be assigned to a ligand-to-metal charge transfer L→Ru (e_g *) transition. These bands are all rather typical of Ru^{II} octahedral polypyridyl complexes.

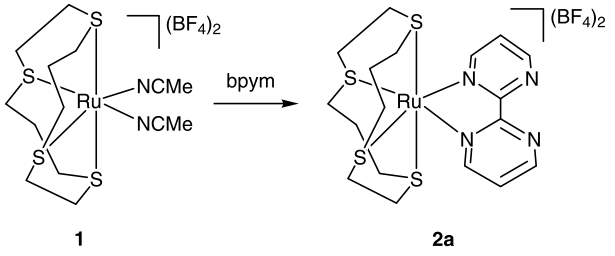

Scheme 1.

The room temperature (r.t.) ^{1}H NMR spectrum of compound **2a** (in CD$_3$NO$_2$ or CD$_3$CN) displays four broad signals in the range 7.9–9.7 ppm for the bpym protons (Table 1), and several broad featureless lines in the range 3.9–2.1 ppm for the protons of the [14]aneS$_4$ macrocycle. For a given solvent, the chemical shift values of the bpym resonances are observed between the downfield shifted bpym signals of the dioxomolybdenum(VI) complex MoCl$_2$O$_2$(bpym) (δ 9.65, 9.37 and 7.97) [12], in which the MoCl$_2$O$_2$ fragment is electron withdrawing, and the upfield shifted signals of the molybdenum(II) compound [CpMo(CO)$_2$(bpym)]BF$_4$ (δ 9.28, 9.15 and 7.66), in which coordination of the bpym ligand to the electron rich organometallic fragment enhances its donor capability [9]. A variable temperature study was carried out for the hexafluorophosphate salt **2b** dissolved in CD$_3$NO$_2$. ^{1}H NMR spectra were measured at 60, 40, 20, 10, 0, −10, −20 and −30 °C. It was found that in the temperature range 40–60 °C the bpym resonances appear as just two signals at 9.25 ppm (doublet of doublets) and 7.91 ppm (triplet). Upon cooling the solution to below r.t., the four broad lines observed at 20 °C begin to resolve and at −30 °C appear as a set of well-defined multiplets (see Section 4). The peaks due to the thioether macrocycle also begin to exhibit structure as soon as the temperature is lowered, and at −30 °C are very well resolved.

Ru *K*-edge EXAFS measurements were carried out at low temperature (30 K) for the compounds [Ru([14]aneS$_4$)(CH$_3$CN)$_2$](BF$_4$)$_2$ (**1**) and [Ru([14]aneS$_4$)(bpym)](BF$_4$)$_2$ (**2a**). The EXAFS data for **1** was fitted by three shells at 2.08, 2.33 and 3.17 Å, corresponding to

Table 1
Selected ^{1}H NMR data at r.t. for bpym and bpym-containing transition metal complexes

Complex	Bpym resonances (ppm)
Bpym	8.96, 7.52 (CD$_3$CN)
[Ru([14]aneS$_4$)(bpym)](BF$_4$)$_2$ (**2a**)	9.72, 9.23, 9.07, 7.92 (CD$_3$NO$_2$)
	9.55, 9.24, 8.84, 7.86 (CD$_3$CN)
[{Ru([14]aneS$_4$)}$_2$(bpym)](BF$_4$)$_4$ (**3**)	9.24, 7.99 (CD$_3$NO$_2$)
	9.11, 7.79 (CD$_3$CN)
[{([14]aneS$_4$)Ru}(bpym){ReO$_3$Me}](BF$_4$)$_2$ (**4**)	9.34, 8.05 (CD$_3$COCD$_3$)
	9.35, 8.10 (CD$_3$NO$_2$)
ReO$_3$Me(bpym) (**5**)	9.11, 7.73 (CD$_3$NO$_2$)
MoO$_2$Cl$_2$(bpym) (**7**) (Ref. [12])	9.67, 9.39, 7.99 (CD$_3$CN)
[CpMo(CO)$_2$(bpym)]BF$_4$ (Ref. [9])	9.28, 9.15, 7.66 (CD$_3$CN)
[{([14]aneS$_4$)Ru}(bpym){MoO$_2$Cl$_2$}](BF$_4$)$_2$	10.0, 8.58 (CD$_3$NO$_2$)

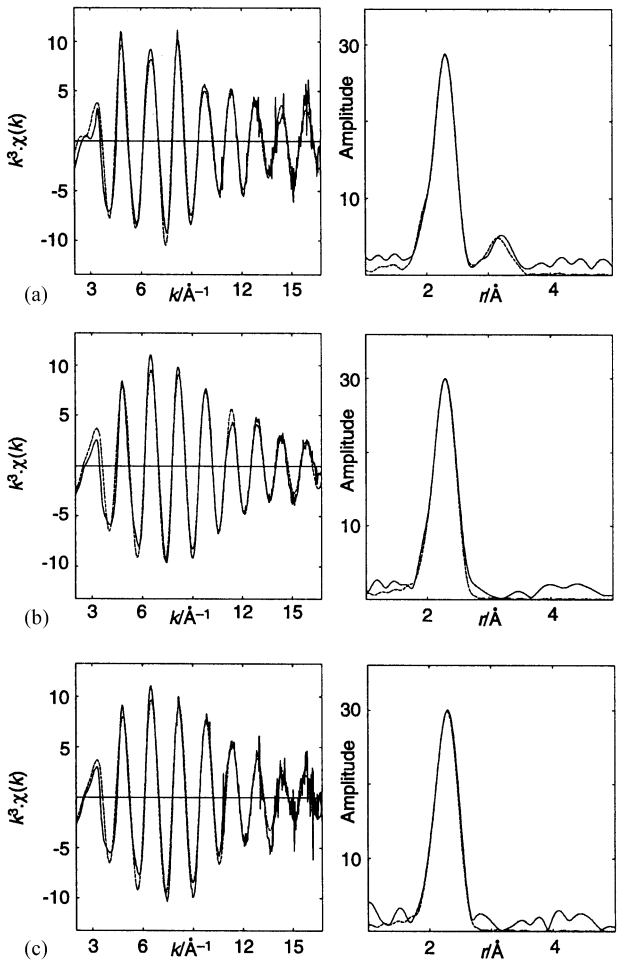

Fig. 1. Ru K-edge k^3-weighted EXAFS and Fourier transforms of (a) [Ru([14]aneS$_4$)(CH$_3$CN)$_2$](BF$_4$)$_2$ (**1**), (b) [Ru([14]aneS$_4$)(bpym)](BF$_4$)$_2$ (**2a**) and (c) [{([14]aneS$_4$)Ru}(bpym){ReO$_3$Me}](BF$_4$)$_2$ (**4**). The solid lines represent the experimental data and the dashed lines show fits using parameters given in Table 2.

Ru–N, Ru–S and Ru···C distances, respectively (Fig. 1, Table 2). The refined coordination numbers indicate that, as expected, the ruthenium atoms in **1** are six-coordinate, comprising four macrocyclic sulfur atoms and two nitrogen atoms from acetonitrile ligands. In order to obtain a satisfactory fit of the third shell for the nitrile carbons, multiple scattering had to be included for the Ru–N–C acetonitrile unit (Ru–N–C = 180°). The EXAFS-derived ruthenium–nitrogen distance is close to those found by single crystal X-ray diffraction for the related [12]aneS$_4$ derivative [Ru([12]-aneS$_4$)(CH$_3$CN)$_2$](BF$_4$)$_2$ (Ru–N = 2.055, 2.086 Å) [14]. Also, the ruthenium–sulfur distance is within the range determined crystallographically for the heterobimetallic compound [Ru([14]aneS$_4$)(4-ferrocenylpyridine)Cl]Cl (2.276–2.339 Å) [10]. Analysis of the Ru K-edge EXAFS of complex **2a** confirms that the bidentate ligand bipyrimidine was successfully introduced into the ruthenium coordination sphere by substitution of the two monodentate acetonitrile ligands in complex **1**. The EXAFS-derived ruthenium–nitrogen (2.14 Å) and ruthenium–sulfur (2.34 Å) distances are in good agreement with those found crystallographically in this work for the same complex (see below). More distant Ru···C distances could not be fitted to the data, possibly due to the crystallographic disorder present.

2.2. Crystal structures of [Ru([14]aneS$_4$)(bpym)](BF$_4$/PF$_6$)$_2$ (2)

The crystal structures of [([14]aneS$_4$)Ru(bpym)](BF$_4$)$_2$ (**2a**) and [([14]aneS$_4$)Ru(bpym)](PF$_6$)$_2$ (**2b**) were determined by X-ray diffraction (Table 3). Selected bond lengths and angles for **2a** are listed in Table 4. The two structures are isostructural and have two cations and four anions in the asymmetric unit. Both structures are disordered. Fig. 2 shows the structure of the ordered cation in **2a** together with the numbering scheme used. The cation has a distorted *cis*-octahedral geometry with S2 and S4 in the plane of the bpym ligand, the [14]aneS$_4$ ligand is folded about the line through S1, Ru1 and S3. In **2a**, three of the four BF$_4^-$ ions are disordered as is one of the cations. The disorder of the cation arises from there being two possible orientations of the [14]aneS$_4$ ligand relative to the plane through Ru(bpym) (Fig. 3). The sites are not equally occupied having occupation factors of 0.680(2) and 0.320. A further form of disorder is that the RuSC$_3$S rings has a twist form whereas all the others have the more stable chair form. The structure of **2b** was studied in the hope that the larger anions would result in a different packing with no disorder. At least the PF$_6^-$ ions are not disordered and it was this structure that gave the clue to the disordering of the [14]aneS$_4$ ligands, since the two sites are more evenly occupied, 0.460(5) and 0.540(5), however, the twist/chair disorder is more prevalent and refinement accounting for all the disorder was not possible.

2.3. Preparation and spectroscopic characterisation of bimetallic complexes

The preparation of the complex [Ru([14]aneS$_4$)(bpym)](BF$_4$)$_2$ (**2**) was also attempted by reaction of the dimethyl sulfoxide adduct [Ru([14]aneS$_4$)(DMSO)Cl]Cl, prepared as described previously [15], with bpym and 2 equiv. of TlBF$_4$ in nitromethane. A dark orange powder was obtained which was washed with ether and recrystallised from nitromethane/diethyl ether. Elemental analysis, IR and ^{1}H NMR indicated that the major product was the binuclear compound [{Ru([14]-aneS$_4$)}$_2$(bpym)](BF$_4$)$_4$ (**3**) (Chart 1). In the r.t. ^{1}H NMR spectrum (CD$_3$CN), the bpym resonances for **3** appear as a doublet at 9.11 ppm and a triplet at 7.79 ppm. The compound could also be prepared by the

Table 2
Ru K-edge and Re L_{III}-edge EXAFS-derived structural parameters

Complex	Edge	Atom	CN [a]	r (Å)	$2\sigma^2$ (Å^2) [b]	E_f (eV) [c]	R (%) [d]
1 [e]	Ru K	S	3.7(3)	2.333(2)	0.0049(3)	−5.8(5)	25.7
		N	2.3(3)	2.081(8)	0.0079(17)		
		C	2.3	3.169(12)	0.0084(22)		
2	Ru K	S	3.9(3)	2.339(3)	0.0049(3)	−6.6(6)	22.5
		N	2.3(4)	2.140(8)	0.0052(13)		
4	Ru K	S	3.9(3)	2.341(3)	0.0047(4)	−6.1(7)	27.0
		N	2.1(4)	2.136(8)	0.0026(11)		
	Re L_{III}	O	2.8(1)	1.734(3)	0.0039(4)	−16.1(6)	24.6
		N	1.8(4)	2.163(11)	0.0136(30)		
5	Re L_{III}	O	2.8(1)	1.729(2)	0.0020(3)	−14.3(5)	21.6
		N	2.2(3)	2.248(8)	0.0107(20)		
		C	4.0(9)	3.206(11)	0.0077(22)		

[a] CN, coordination number. Values in parentheses are statistical errors generated in EXCURVE. The true errors in coordination numbers are likely to be of the order of 20%; those for the interatomic distances approximately 1.5% [13].
[b] Debye–Waller factor; σ = root-mean-square internuclear separation.
[c] E_f = edge position (Fermi energy), relative to calculated vacuum zero.
[d] $R = (\int[\Sigma^{theory} - \Sigma^{exptl}]k^3 dk / [\Sigma^{exptl}]k^3 dk) \times 100\%$.
[e] Multiple scattering calculation for Ru–N–C: Ru–N–C = 180°; maximum path-length = 10 Å; maximum order of scattering = 3; paths considered = Ru–N–C–Ru, Ru–N–C–N–Ru, Ru–C–N–C–Ru.

Table 3
Crystal data and details of structure refinement for [Ru([14]aneS$_4$)(bpym)](BF$_4$)$_2$ (**2a**) and [Ru([14]aneS$_4$)(bpym)](PF$_6$)$_2$ (**2b**)

	2a	**2b**
Molecular formula	$C_{18}H_{26}B_2F_8N_4S_4Ru$	$C_{18}H_{26}F_{12}N_4P_2S_4Ru$
M	701.44	793.73
Crystal system	monoclinic	monoclinic
Space group	$P2_1/n$	$P2_1/n$
a (Å)	16.454(1)	17.104(1)
b (Å)	19.830(2)	20.524(1)
c (Å)	17.300(1)	17.524(1)
β (°)	115.414(1)	115.143(1)
V (Å^3)	5098(1)	5574.3(6)
Z	8	8
T (K)	120	120
μ (mm^{-1})	1.019	1.074
Measured reflections	70 343	72208
Unique reflections (R_{int})	14 096 (0.048)	16 753 (0.138)
2θ Range (°)	2.3–29.8	2.2–29.8
R_1	0.041	0.070
wR_1 ($I > 3\sigma I$)	0.040	0.065

Table 4
Selected bond lengths (Å) and angles (°) for [Ru([14]aneS$_4$)(bpym)](BF$_4$)$_2$ (**2a**)

Bond lengths			
Ru1–N1	2.123(3)	Ru1–S1	2.349(1)
Ru1–N4	2.101(3)	Ru1–S2	2.309(1)
		Ru1–S3	2.345(1)
		Ru1–S4	2.314(1)
Bond angles			
N1–Ru1–N4	78.0(1)	S1–Ru1–S2	94.56(3)
N1–Ru1–S1	92.04(8)	S1–Ru1–S3	176.88(4)
N1–Ru1–S2	167.06(8)	S1–Ru1–S4	82.52(3)
N1–Ru1–S3	88.55(8)	S2–Ru1–S3	85.47(3)
N1–Ru1–S4	102.52(8)	S2–Ru1–S4	89.38(3)
N4–Ru1–S1	93.81(8)	S3–Ru1–S4	94.36(3)
N4–Ru1–S2	90.44(8)		
N4–Ru1–S3	89.31(8)		
N4–Ru1–S4	176.30(8)		

reaction of the acetonitrile adduct **1** with 1 equiv. of the bpym adduct **2a**. A similar [9]aneS$_3$ bimetallic compound, formulated as [{Ru([9]aneS$_3$)Cl}$_2$(bpym)](PF$_6$)$_2$, was recently reported [3].

The successful preparation of the Ru$^{II}\cdots$Ru^{II} bimetallic complex **3** led us to investigate further the donor capability of the bpym ligand when coordinated to the [Ru([14]aneS$_4$)]$^{2+}$ fragment (compound **2**), in particular for the formation of heterobinuclear adducts with oxorhenium(VII) and oxomolybdenum(VI) fragments. Addition of methyltrioxorhenium(VII) (MTO) to a solution of **2a** in nitromethane gave a brown–violet precipitate, identified as the heterobinuclear adduct [{([14]aneS$_4$)Ru}(bpym){ReO$_3$Me}](BF$_4$)$_2$ (**4**). MTO is known to form octahedral adducts with many bidentate Lewis bases, including bipyrimidine [16]. The bridging ligand in **4** gives rise to two lines in the ^{1}H NMR spectrum at 9.34 and 8.05 ppm. The ^{1}H NMR chemical shift for the Re–CH$_3$ group in **4** is located at 2.07 ppm, close to that observed for ReO$_3$Me(bpym) (**5**) (2.10 ppm, 20 °C, CD$_3$NO$_2$). The shifts in these resonances compared to that of un-coordinated MTO [$\delta_H = 2.67$] are a consequence of electron donation to the Lewis acidic metal centre. Concerning the IR spectrum of compound **4**, two bands are observed at 1574 and 1549 cm^{-1} due to C=C and C=N pyrimidine ring stretching vibrations, very similar to those exhibited by the adducts

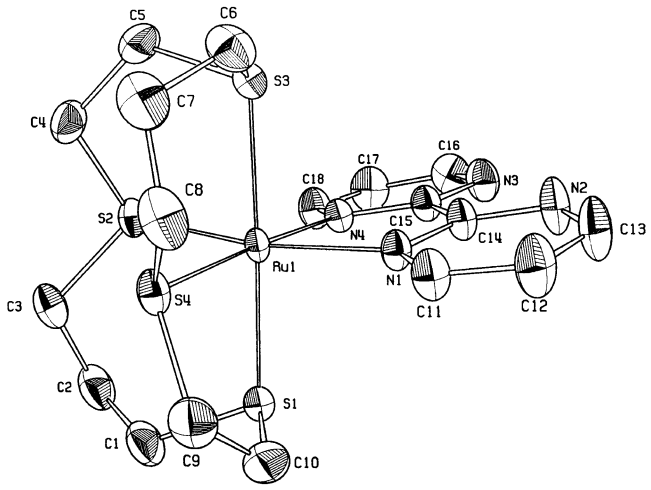

Fig. 2. Molecular structure of the ordered cation for [([14]aneS$_4$)Ru(bpym)](BF$_4$)$_2$ (**2a**), with labelling scheme. Thermal ellipsoids are drawn at the 50% probability level and hydrogen atoms have been omitted for clarity.

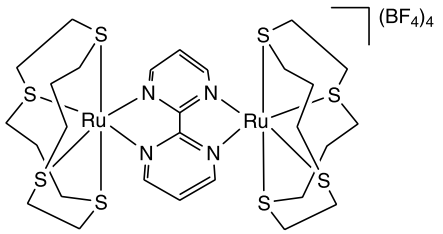

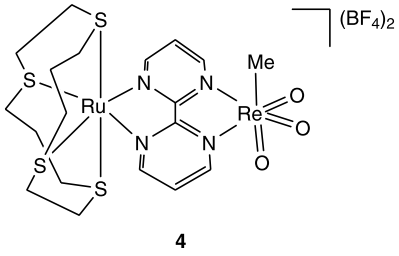

4

1.

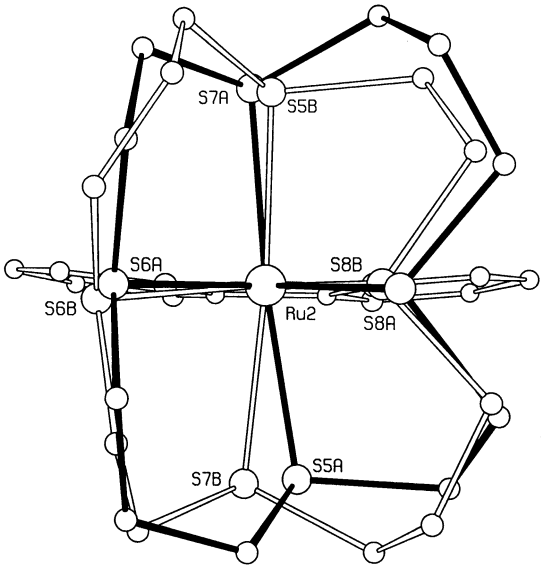

Fig. 3. Molecular structure of the disordered cation for [([14]aneS$_4$)Ru(bpym)](BF$_4$)$_2$ (**2a**); atoms are represented by spheres of arbitrary size with Ru as the largest circles and S as the next largest. The [14]aneS$_4$ ligand with occupation 0.680(2), A, is drawn with filled bonds and that with occupation 0.320, B, with open bonds.

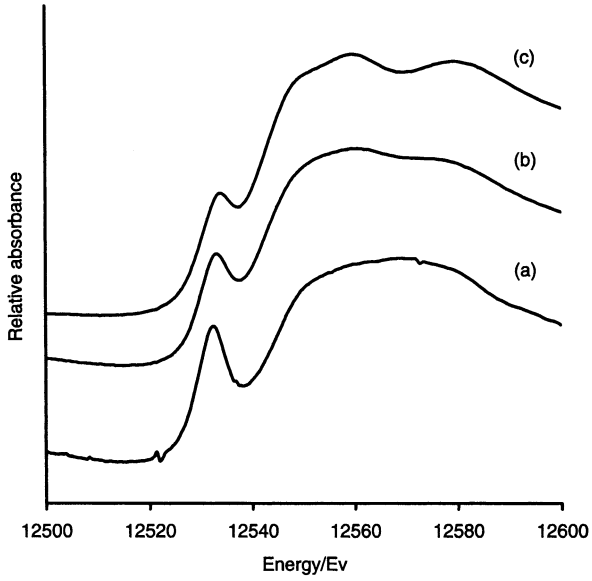

Fig. 4. Re L_I-edge XANES spectra of (a) MTO, (b) ReO$_3$Me(bpym) (**5**) and (c) [{([14]aneS$_4$)Ru}(bpym){ReO$_3$Me}](BF$_4$)$_2$ (**4**).

2 and **5**. Ru *K*-edge EXAFS analysis for complex **4** indicates that the ruthenium local coordination sphere (up to 5 Å from the absorber) is largely unchanged compared to that for complex **2a** (Table 2, Fig. 1). There was no evidence for a well-defined ruthenium···rhenium outer coordination shell, although this is not surprising since the metal–metal distance must be close to 5.5 Å.

Fig. 4 shows the Re L_I X-ray absorption near edge structure (XANES) spectra of MTO, ReO$_3$Me(bpym) (**5**) and the complex [{([14]aneS$_4$)Ru}(bpym){ReO$_3$Me}](BF$_4$)$_2$ (**4**). The XANES spectrum of MTO contains an intense pre-edge peak, caused by a 2s → 5d(Re) + 2p(O) electron transition [17]. With respect to the rhenium coordination, the intensity of this peak is usually strongest for systems with non-inversion symmetry, such as tetrahedral coordination. Any distortion of the regular tetrahedral symmetry leads to a decrease in the peak intensity [18]. The pre-edge peak for compounds **4** and **5** is less intense than that for MTO, consistent with a change from tetrahedral to distorted octahedral symmetry. It is also evident that, towards higher energy, the XANES for **4** and **5** are quite similar, while MTO exhibits a quite different set of oscillations in the absorption coefficient. This is a very good

indication that the local coordination environment of rhenium in compound **4** is similar to that in compound **5**.

Analysis of the Re L_{III} EXAFS spectrum of the Lewis base adduct **5** allowed three shells for O, N and C neighbours to be determined, in order of increasing distance from the absorbing atom (Table 2, Fig. 5). The Re–O bond distance of 1.73 Å is typical of all known Re^{VII} oxo complexes containing a Re=O double bond [19]. Bidentate coordination of the bipyrimidine ligand is confirmed by the presence of the other two shells for N(2.25 Å) and C(3.21 Å). The Re–N bond distance is comparatively long, indicating a weak N→Re bonding interaction. Identical Re–N bond distances were determined by single crystal X-ray crystallography for the adducts $XReO_3$·[4,4′-bis(*tert*-butyl)-2,2′-bipyridine] (X = Cl, Br) [20]. It was not possible to fit a fourth shell for the methyl carbon atom, expected at about 2.1 Å. This may be due to the close proximity of this shell with the nitrogen shell, coupled with the fact that the two elements have very similar back-scattering properties. The Re L_{III} EXAFS of complex **4** was initially fitted by a model comprising one shell of oxygen atoms. Both the refined distance [1.733(3) Å] and coordination number [2.8(2)] are consistent with the presence of trioxorhenium species. Addition of a second shell for nitrogens at 2.16 Å (coordination number = 1.8) reduced the *R*-factor from 31.6 to 24.6% (Table 2, Fig. 5). This shell was significant at the 99% level according to the statistical test of Joyner et al. [21]. However, the distance is significantly shorter than that determined for

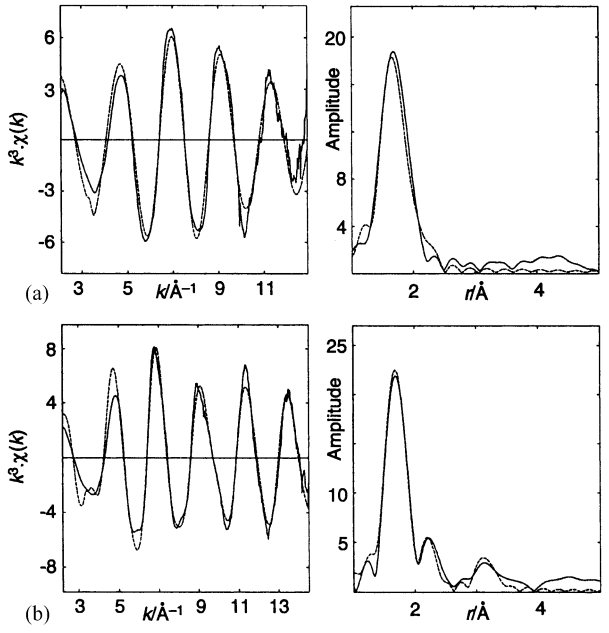

Fig. 5. Re L_{III}-edge k^3-weighted EXAFS and Fourier transforms of (a) [{([14]aneS$_4$)Ru}(bpym){ReO_3Me}]$(BF_4)_2$ (**4**) and (b) ReO_3Me(bpym) (**5**). The solid lines represent the experimental data and the dashed lines show fits using parameters given in Table 2.

complex **5**. This may be due to the influence of the carbon shell at about 2.1 Å.

Complexes **2a**, **4** and **5**, and MTO, were examined by thermogravimetry (TG). The precursor ruthenium complex **2a** decomposes in two steps (DTG_{max} = 323 and 408 °C), the onset temperature of the first decomposition step being 230 °C. At 900 °C, 14% remains as residual weight. Two steps are observed in the thermal decomposition of the adduct **5**, characterised by DTG maximums at 113 and 420 °C. The first step, which begins at about 75 °C, must correspond to rupture of the Re–N bond and sublimation of the now un-coordinated MTO. Pure MTO sublimes below 100 °C under TG conditions. Therefore, coordination of MTO to bpym does not improve its thermal stability to a significant degree. After the second step, 100% mass loss is complete at 550 °C. The adduct **4** decomposes in several steps up to 900 °C, the first two of which coincide with the first decomposition steps observed for **2a** and **5**. At 900 °C, 12.8% remains as residual weight.

Like MTO, dioxomolybdenum(VI) fragments of the type MoO_2X_2 (X = Cl, Br, Me) are known to form octahedral Lewis base adducts of the type MoO_2X_2L with bidentate ligands such as bipyrimidine [12]. An attempt to prepare a heterobinuclear ligand-bridged $Ru^{II}\cdots Mo^{VI}$ complex was made by the reaction of [Ru([14]aneS$_4$)(bpym)]$(BF_4)_2$ (**2a**) with the tetrahydrofuran adduct $MoO_2Cl_2(THF)_2$ (**6**) in nitromethane. A deep red solution formed immediately. The crude product isolated from this reaction did indeed contain the desired binuclear complex (as evidenced by ^{1}H NMR, Table 1), but only as a minor component. Attempts to purify the mixture were unsuccessful. The reaction was also carried out starting from the acetonitrile complex [Ru([14]aneS$_4$)$(CH_3CN)_2$]$(BF_4)_2$ (**1**) and the adduct MoO_2Cl_2(bpym) (**7**). However, once again, the binuclear complex was only formed in a small quantity.

3. Concluding remarks

The Ru^{II} thioether complex [Ru([14]aneS$_4$)(bpym)]$(BF_4)_2$ is readily prepared from the dication [Ru([14]aneS$_4$)$(CH_3CN)_2$]$^{2+}$. This complex, in which ruthenium is stabilised in a low oxidation state by the macrocyclic thioether ligand, can act as a 'metalloligand' and bind other metals at the free coordination site. This allows the formation of the symmetric bimetallic system [{Ru([14]aneS$_4$)}$_2$(bpym)]$^{4+}$ and also heterobimetallic complexes in which one metal is in a low oxidation state (Ru^{II}) and the other is in a high oxidation state (Re^{VII}), e.g. [{([14]aneS$_4$)Ru}(bpym){ReO_3Me}]$^{2+}$.

4. Experimental

4.1. General procedures and starting materials

All preparations and manipulations were performed using standard Schlenk techniques under nitrogen. Commercial grade solvents were dried and deoxygenated by refluxing with appropriate drying agents under nitrogen and distilled prior to use. Literature methods were used to prepare the compounds [Ru([14]aneS$_4$)(DMSO)Cl]Cl [15], [Ru([14]aneS$_4$)(CH$_3$CN)$_2$](BF$_4$)$_2$ (**1**) [10], methyl(2,2′-bipyrimidine)trioxorhenium (**5**) [16], $MoO_2Cl_2(THF)_2$ (**6**) [9], and MoO_2Cl_2(bpym) (**7**) [12].

Microanalyses were obtained with a LECO CHNS-932 Elemental Analyser. TGA studies were performed using a Shimadzu TGA-50 system at a heating rate of 5 K min^{-1} under a nitrogen atmosphere. IR spectra were obtained as KBr pellets using a FTIR Mattson-7000 infrared spectrophotometer. Raman spectra were recorded on a Bruker RFS 100/S FT Raman spectrometer using a 1064 nm excitation of the Nd/YAG laser. UV–Vis spectra were obtained at r.t. with a JASCO V-560 spectrophotometer. ^{1}H NMR spectra were recorded on a Bruker AMX-300 spectrometer.

Ru *K*-edge and Re *L*-edge X-ray absorption spectra were measured at approximately 30 K (using an Oxford Instruments cryostat filled with He exchange gas) in transmission mode on beamline BM29 at the ESRF (Grenoble) [22], operating at 6 GeV in 2/3 filling mode with typical currents of 170–200 mA. One scan was performed for each sample and set up to record the pre-edge at 5 eV steps and the post-edge region in 0.025–0.05 Å^{-1} steps, giving a total acquisition time of approximately 45 min per scan. The order-sorting double Si(3 1 1) crystal monochromator was detuned by 40% for harmonic rejection. Solid samples were diluted with BN and pressed into 13-mm pellets. Air-sensitive samples were handled under an inert gas. Ionisation chamber detectors were filled with Ar to give 30% absorbing I_o (incidence) and 70% absorbing I_t (transmission). The programs EXCALIB and EXBACK (SRS Daresbury Laboratory, UK) were used in the usual manner for calibration and background subtraction of the raw data. EXAFS curve-fitting analyses, by least-squares refinement of the non-Fourier filtered k^3-weighted EXAFS data, were carried out using the program EXCURVE (version EXCURV-98 [23]) using fast curved wave theory [24,25]. Phase shifts were obtained within this program using ab initio calculations based on the Hedin Lundqvist/von Barth scheme. Unless otherwise stated, the calculations were performed with single scattering only.

4.2. Syntheses

4.2.1. [Ru([14]aneS$_4$)(bpym)](BF$_4$)$_2$ (**2a**)

A solution of [Ru([14]aneS$_4$)(CH$_3$CN)$_2$](BF$_4$)$_2$ (**1**) (1.01 g, 1.61 mmol) in dry ethanol (40 ml) was treated with bpym (0.51 g, 3.22 mmol). After refluxing for 72 h, the solution was evaporated to dryness to give an orange powder. The crude product was washed with ether and recrystallised from ethanol/ether (1.05 g, 93%). Selected IR (KBr): ν_{max} = 3086m, 2961m, 2919m, 2851w, 1574s, 1550m, 1437sh, 1416s, 1402vs, 1366w, 1300m, 1070vs, 1030vs, 954sh, 860m, 818m, 752s, 685m, 663m, 642m, 533s, 522s, 458w cm^{-1}. Selected FT Raman: 3107w, 2932vs, 1577s, 1552m, 1467s, 1419w, 1336m, 1208m, 1106w, 1021s, 786m, 685w, 643m, 605w, 374w, 334w, 301m cm^{-1}. UV–Vis (CH$_3$CN): λ_{max}/nm ($\varepsilon \times 10^{-3}$ M^{-1} cm^{-1}) = 415sh (2.15), 332 (4.04), 264 (12.77), 239sh (12.46), 201 (38.05). ^{1}H NMR (300 MHz, CD$_3$NO$_2$, SiMe$_4$, 20 °C): δ = 9.72 (br, bpym), 9.23 (br, bpym), 9.07 (br, bpym), 7.92 (m, bpym), 3.80–3.40 (m, [14]aneS$_4$), 3.30–2.80 (m, [14]aneS$_4$), 2.75–2.45 (br, [14]aneS$_4$), 2.40–2.10 (m, [14]aneS$_4$). $C_{18}H_{26}B_2F_8N_4RuS_4$ (701.4): Calc. C 30.83, H 3.74, N 7.99. Found: C 30.72, H 3.64, N 7.90%.

The hexafluorophosphate salt **2b** was prepared as follows: A saturated aqueous solution of LiCl (2 ml) was added to a solution of **2a** (0.15 g, 0.21 mmol) in acetone (10 ml). The resulting orange precipitate was isolated by filtration, rinsed with water/acetone and dried in vacuo. A saturated aqueous solution of NH_4PF_6 (2 ml) was then added to a solution of the chloride salt in ethanol. A yellow precipitate formed, which was isolated by filtration, rinsed with ethanol/diethyl ether and dried in vacuo. The product was recrystallised from acetonitrile/diethyl ether. ^{1}H NMR (300 MHz, CD$_3$NO$_2$, SiMe$_4$, 20 °C): δ = 9.72 (br, bpym), 9.23 (br, bpym), 9.06 (br, bpym), 7.90 (m, bpym), 4.00–3.60 (m, [14]aneS$_4$), 3.40–2.90 (m, [14]aneS$_4$), 2.90–2.55 (br, [14]aneS$_4$), 2.30–2.20 (m, [14]aneS$_4$). ^{1}H NMR (300 MHz, CD$_3$NO$_2$, SiMe$_4$, 60 °C): δ = 9.26 (dd, bpym), 7.91 (t, bpym), 3.70–3.35 (br, [14]aneS$_4$), 3.35–3.20 (m, [14]aneS$_4$), 3.20–2.90 (m, [14]aneS$_4$), 2.90–2.65 (m, [14]aneS$_4$), 2.60–2.30 (br, [14]aneS$_4$). ^{1}H NMR (300 MHz, CD$_3$NO$_2$, SiMe$_4$, −30 °C): δ = 9.73 (dd, bpym), 9.20 (m, bpym), 9.05 (dd, bpym), 7.90 (m, bpym), 3.93–3.80 (m, [14]aneS$_4$), 3.75–3.65 (m, [14]aneS$_4$), 3.33–2.95 (m, [14]aneS$_4$), 2.81–2.60 (m, [14]aneS$_4$), 2.44–2.35 (m, [14]aneS$_4$), 2.25–2.00 (m, [14]aneS$_4$).

4.2.2. [{Ru([14]aneS$_4$)}$_2$(bpym)](BF$_4$)$_4$ (**3**)

A solution of **2a** (0.22 g, 0.31 mmol) in nitromethane (10 ml) was added to a stirred solution of **1** (0.22 g, 0.31 mmol) in nitromethane (10 ml). The resulting dark orange solution was refluxed for 48 h, then cooled to r.t. and diethyl ether added to precipitate a dark orange powder (0.27 g, 70%). Selected IR (KBr): ν_{max} = 2926w,

1574s, 1555m, 1433sh, 1402vs, 1300m, 1066vs, 1030vs, 860m, 818m, 752s, 685m, 662m, 643m, 533s, 522s, 457w cm^{-1}. ^1H NMR (300 MHz, CD_3NO_2, $SiMe_4$, 20 °C): $\delta = 9.24$ (d, bpym), 7.99 (t, bpym), 4.00–3.55 (m, [14]aneS$_4$), 3.50–2.90 (m, [14]aneS$_4$), 2.90–2.58 (m, [14]aneS$_4$), 2.55–2.30 (m, [14]aneS$_4$), 2.30–2.05 (m, [14]aneS$_4$). $C_{28}H_{46}N_4B_4F_{16}S_8Ru_2$ (1244.6): Calc. C, 27.02; H, 3.73; N, 4.50. Found: C, 27.38; H, 3.64; N, 4.47%.

4.2.3. [{([14]aneS$_4$)Ru}(bpym){ReO$_3$Me}](BF$_4$)$_2$ (**4**)

A solution of methyltrioxorhenium (0.06 g, 0.24 mmol) in nitromethane (5 ml) was added to a solution of **2a** (0.11 g, 0.16 mmol) in nitromethane (10 ml) and the mixture stirred at r.t. for 24 h. The colourless solution was filtered off and the remaining red–orange precipitate washed three times with 10 ml portions of hexane, 10 ml of diethyl ether, and dried under reduced pressure (0.14 g, 92%). Selected IR (KBr): $\nu_{max} = 2920$m, 1574s, 1549m, 1401vs, 1286m, 1070vs, 1029vs, 939m, 908m, 861w, 818m, 752s, 662m, 521s cm^{-1}. ^1H NMR (300 MHz, CD_3COCD_3, $SiMe_4$, 20 °C): $\delta = 9.34$ (d, bpym), 8.05 (br, bpym), 4.00–3.20 (m, [14]aneS$_4$), 2.95–2.55 (m, [14]aneS$_4$), 2.15–2.00 (m, [14]aneS$_4$), 2.07 (s, MTO). $C_{19}H_{29}B_2F_8N_4O_3ReRuS_4$ (950.6): Calc. C, 24.01; H, 3.08; N, 5.89. Found: C, 24.29; H, 3.03; N, 5.62%.

4.3. X-ray crystallography

The crystal data and structure refinement details are given in Table 3. Data for the two complexes **2a** and **2b** were measured on a Siemens SMART diffractometer using graphite monochromated Mo Kα radiation ($\lambda =$ 0.71073 Å). Data were corrected for Lorentz-polarisation effects and for absorption [26]. In the case of **2a**, one of the two cations and three of the four BF_4^- anions in the asymmetric unit were disordered. The disorder of the cation arises from there being two ways in which the [14]aneS$_4$ moiety can coordinate to the Ru(bpym) unit (see Section 2). The two possible orientations are approximately related by reflection in the plane defined by the bpym ligand. In the least-squares refinement all of the [14]aneS$_4$ groups were originally constrained to be identical [27], however, two carbon atoms of the least-occupied ligand site, C19B and C20B, were found to be further disordered so that the $RuSC_3S$ ring has the twist form instead of the chair form. In the final refinement, while the rest of ligand B was constrained to be identical to the ordered ligand, C19B and C20B were refined using slack restraints. Hydrogen atoms were kept fixed in calculated positions with C–H = 0.95 Å and $U_{iso} = 1.2U_{eq}$ for the atom to which they were bonded. The disordered BF_4^- ions were constrained to be tetrahedral and a mean B–F distance was refined. The structure of **2b** is very similar to that of **2a**; whilst the PF_6^- ions are ordered the cations are disordered, both by the reflection of the ligand in the plane of the bpym ligand for one cation and apparently by chair–twist disorder for both cations. It was not possible to refine both types of disorder hence the resulting high R-value and unrealistically short C–C distances and large C–C–C angle in the six-membered rings.

5. Supplementary material

CCDC-207461 (**2a**) and CCDC-207462 (**2b**) contain the supplementary crystallographic data for this paper. These data can be obtained free of charge at http://www.ccdc.cam.ac.uk/conts/retrieving.html or from the Cambridge Crystallographic Data Centre, 12 Union Road, Cambridge CB2 1EZ, UK (fax: +44-1223-336033; e-mail: deposit@ccdc.cam.ac.uk).

Acknowledgements

This work was partly funded by FCT, POCTI and FEDER (Project POCTI//QUI/37990/2001). We acknowledge the European Synchrotron Radiation Facility for provision of synchrotron radiation facilities and we would like to thank Silvia Ramos for assistance in using beamline BM29. C.N. and J.M. thank the University of Aveiro and PRAXIS XXI, respectively, for research grants. A.H. and J.J. are indebted to the Carlsberg Foundation for the diffractometer and the cooling device.

References

[1] V. Balzani, A. Juris, M. Venturi, S. Campagna, S. Serroni, Chem. Rev. 96 (1996) 759.
[2] S.M. Scott, K.C. Gordon, Inorg. Chim. Acta 254 (1997) 267.
[3] C.S. Araújo, M.G.B. Drew, V. Félix, L. Jack, J. Madureira, M. Newell, S. Roche, T.M. Santos, J.A. Thomas, L. Yellowlees, Inorg. Chem. 41 (2002) 2250.
[4] D.P. Rillema, R. Sahai, P. Matthews, A.K. Edwards, R.J. Shaver, L. Morgan, Inorg. Chem. 29 (1990) 167.
[5] G.N.A. Nallas, S.W. Jones, K.J. Brewer, Inorg. Chem. 35 (1996) 6974.
[6] F. Baumann, A. Stange, W. Kaim, Inorg. Chem. Commun. 1 (1998) 305.
[7] G.D. Munno, T. Poerio, M. Julve, F. Lloret, J. Faus, A. Caneschi, J. Chem. Soc., Dalton Trans. (1998) 1679.
[8] M.G.B. Drew, V. Félix, I.S. Gonçalves, F.E. Kühn, A.D. Lopes, C.C. Romão, Polyhedron 17 (1998) 1091.
[9] F.E. Kühn, E. Herdtweck, J.J. Haider, W.A. Herrmann, I.S. Gonçalves, A.D. Lopes, C.C. Romão, J. Organomet. Chem. 583 (1999) 3.
[10] C.D. Nunes, T.M. Santos, H.M. Carapuça, A. Hazell, M. Pillinger, J. Madureira, W.-M. Xue, F.E. Kühn, I.S. Gonçalves, New J. Chem. 26 (2002) 1384.

[11] B.J. Goodfellow, S.M.D. Pacheco, J.P. de Jesus, V. Félix, M.G.B. Drew, Polyhedron 16 (1997) 3293.
[12] F.E. Kühn, M. Groarke, É. Bencze, E. Herdtweck, A. Prazeres, A.M. Santos, M.J. Calhorda, C.C. Romão, I.S. Gonçalves, A.D. Lopes, M. Pillinger, Chem. Eur. J. 8 (2002) 2370.
[13] J. Evans, J.T. Gauntlett, J.F.W. Mosselmans, Faraday Discuss. Chem. Soc. 89 (1990) 107.
[14] T.M. Santos, B.J. Goodfellow, J. Madureira, J.P. de Jesus, V. Félix, M.G.B. Drew, New J. Chem. 23 (1999) 1015.
[15] M. Pillinger, I.S. Gonçalves, A.D. Lopes, J. Madureira, P. Ferreira, A.A. Valente, T.M. Santos, J. Rocha, J.F.S. Menezes, L.D. Carlos, J. Chem. Soc., Dalton Trans. (2001) 1628.
[16] P. Ferreira, W.-M. Xue, E. Bencze, E. Herdtweck, F.E. Kühn, Inorg. Chem. 40 (2001) 5834.
[17] M. Fröba, K. Lochte, W. Metz, J. Phys. Chem. Solids 57 (1996) 635.
[18] M. Fröba, O. Muth, Adv. Mater. 11 (1999) 564.
[19] C.C. Romão, F.E. Kühn, W.A. Herrmann, Chem. Rev. 97 (1997) 3197.
[20] F.E. Kühn, J.J. Haider, E. Herdtweck, W.A. Herrmann, A.D. Lopes, M. Pillinger, C.C. Romão, Inorg. Chim. Acta 279 (1998) 44.
[21] R.W. Joyner, K.J. Martin, P. Meehan, J. Phys. C 20 (1987) 4005.
[22] A. Filipponi, M. Borowski, D.T. Bowron, S. Ansell, A.D. Cicco, S.D. Panfilis, J.-P. Itiè, Rev. Sci. Instrum. 71 (2000) 2422.
[23] N. Binsted, EXCURV98, CCLRC Daresbury Laboratory computer programme, 1998.
[24] S.J. Gurman, N. Binsted, I. Ross, J. Phys. C 17 (1984) 143.
[25] S.J. Gurman, N. Binsted, I. Ross, J. Phys. C 19 (1986) 1845.
[26] Siemens, SMART, SAINT and XPREP Area-Detector Control and Integration Software, Siemens Analytical X-ray instruments Inc., Madison, WI, USA, 1995.
[27] G.S. Pawley, Adv. Struct. Res. 4 (1971) 1.